CFD simulation of a rotary compressor with gas injection

IOP Conf. Series: Materials Science and Engineering **604** (2019) 012084 doi:10.1088/1757-899X/604/1/012084

CFD simulation of a rotary compressor with gas injection

Junfeng Wang[1], Hui Ding[1], Baolong Wang[2], Yunchen Ding[2] and Yanfen Huang[3]

[1] Simerics Inc., Bellevue, WA, USA
[2] Tsinghua University, Beijing, China
[3] Beijing Hi-key Tech Co.Ltd, Beijing, China

E-mail: jw@simerics.com, Wangbl@tsinghua.edu.cn

Abstract. Rotary compressors are widely used in small capacity refrigeration and heat pump Systems. Gas injection is an effective way to improve compressor efficiency especially when operating under low temperature. A novel design injects gas through the rotary compressor blade, controlled by a built in reed valve. CFD simulation provides valuable insights to help design engineers to verify, to analyze, and to improve the performance of compressors. For this particular application, besides modeling rotary compressor operation, CFD simulation also needs to solve reed valve dynamics with combined movement of the blade. In this paper, a full 3D transient CFD model of a rotary compressor with gas injection is described in detail. Real gas properties is used for the refrigerant. Methodology used to model reed valve dynamics is discussed. Simulation results are validated by experiment data. Effects of gas injection are evaluated by comparing the simulation results for the cases with and without gas injection.

1. Introduction

Rotary piston type compressors are widely used in air-conditioning and refrigerating systems because of their compact size, high volumetric efficiency, low noise and high reliability. However, in cold regions, the low ambient temperature will result in a severe performance degradation of air source heat pumps with rotary compressors due to the lower mass flow rate [1]. Among many solutions aiming at improving the pump performance in such situation, econonizer technology has gained its popularity due to its efficiency and low cost [2, 3]. In a compression system with an economizer, the refrigerant gas in a secondary loop is injected into the compression pocket through the so-called gas injection port. Gas injection has been widely investigated and applied to scroll compressors, screw compressors [4, 5, 6] and twin-cylinder rotary compressor [7, 8]. For the single-cylinder rotary compressor with a gas injection system, recent experiments [9, 10] also showed an enhanced performance under low ambient temperature environment. The gas injection port in a single-cylinder rotary compressor for a traditional design is opened on the cylinder wall and close to the discharge port for a longer injection time and higher refrigerant rate. However, such design will cause unavoidable back flow of the injection refrigerant into the suction tube, which will diminish the merits of the gas injection. Wang *et al.* [11] proposed a novel gas injection structure, in which the injection passage is screwed in the middle of a platform on the blade where the spring valve plate and the lift limiter are installed as shown in

Figure 1. This new design can avoid the back flow and achieve maximum of the injection mas flow.

In order to investigate the performance of the new injection design, a full 3D transient Computational Fluid Dynamics (CFD) simulation is desired, especially when the rotary piston compressor is coupled with control valves . CFD simulations of combined compressor and valve systems can provide valuable insights regarding not only the performance of the compressor and the valve, but also the dynamic interaction between the two.

CFD simulation of a rotary piston compressor can be traced back to 1994 when Lenz and Cooksey used steady state CFD solution to optimize the discharge port geometry. Geng [12] and Liang [13] further extended the rolling piston CFD models to a more accurate transient moving mesh approach. In those two models, the reed valve lifts were simplified as a simple function of pressure difference without considering the complex valve dynamic behavior under fluid forces. More detailed approaches have been used in reed valve studies. Machu [14] used finite element methods to model detailed deformation of a reed valve with a pre-defined flow field. Silva [15] solved an ODE for valve dynamics within a 1D fluid model. Kinjo [16] used immersed solid/virtual flux to account for the motion of the valves of a reciprocating compressor inside a simplified fluid domain, together with ODEs to model valve dynamics.

In this paper, the commercially available package Simerics-MP+ is employed to perform the full 3D transient CFD simulations, in which the rotary piston compressor and reed valves are fully coupled and treated as a complete system disscussed earlier by Ding and Gao[18].

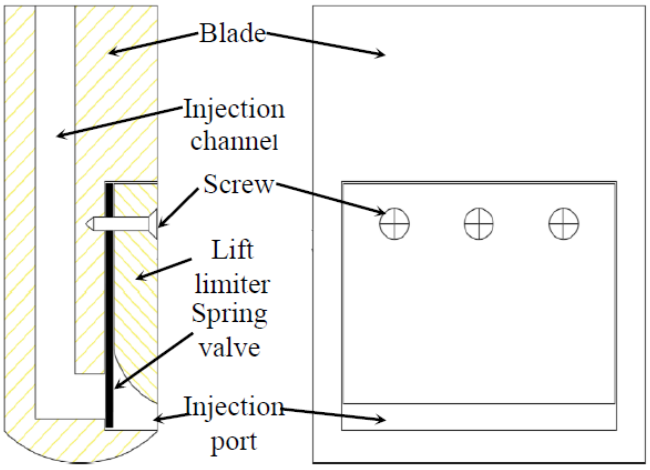

Figure 1. Schematic of the blade with gas injection structure

2. Rotary piston model and mesh solution

A rotary piston consists of a cylindrical rotor mounted eccentrically on a driving shaft and assembled inside a cylinder chamber. The space between the rotor and the chamber is divided into a suction chamber (low pressure) and a compression chamber (high pressure) by a moving vane. With the rotation of the piston, the volume of the compression chamber is reduced. Once the pressure is built sufficient high, the discharge valve will be forced to open to allow the gas to exit.

Rotary piston mesh is automatically created by the template named *Rolling Piston* in the commercial available package based a user defined rotor, chamber and vane tip geometry. The

template also controls the rotor movement with user defined operating conditions and updates the mesh at every time step in a transient simulation. Figure 2 shows a typical rotary piston mesh which consists of a main chamber mesh and vane tip mesh. More details for the rotary piston model are discussed in [18].

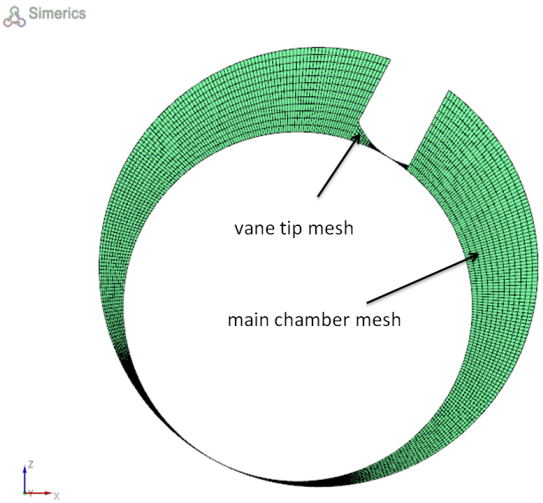

Figure 2. Sectional view of a typical rotary piston mesh

3. Reed vavlve model and dynamics

An example of reed valve is shown Figure 3(a): it is typically made of thin layer of metal with one end fixed and the other end free. Under sufficient fluid force in the opening direction, the valve will bend and open to allow the fluid to flow through the opening. If fluid force is in the other direction, the valve will be pushed to close the flow channel.

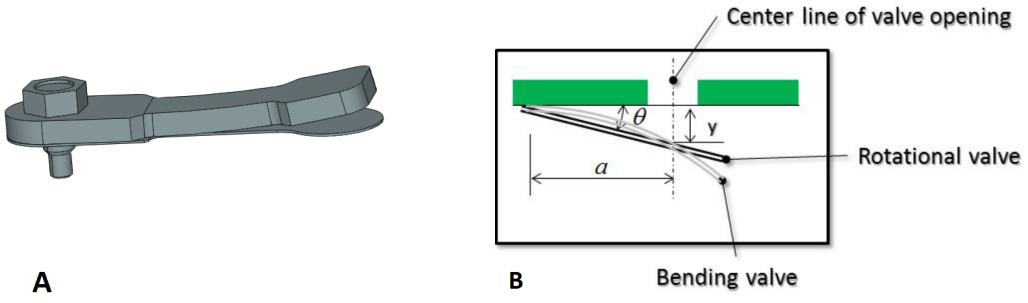

Figure 3. (A) Reed valve (B) Rotation vs bending of the reed valve

The reed valve movement is modeled as a rotation around its fixed end as shown in Figure 3(b). This approach is a more accurate approximation of the real valve bending compared with a 1D linear valve motion model, without coupling to a complex strain-stress analysis. The valve reed dynamics is thus modeled as a torsional mass and spring system described by the following ODE:

$$I\frac{d^2\theta}{dt^2} + C\frac{d\theta}{dt} + K\theta = T(t) \tag{1}$$

where θ is the valve opening angle starting from the valve closed position, I is the moment of inertia, C is the rotational friction, K is the coefficient of torsion spring, T is the torque from fluid forces, and t is time. The value of the torsion coefficient is defined by angular form of Hooker's law:

$$K = \frac{T}{\theta} \tag{2}$$

And the torsion coefficient can be derived by matching the rotational motion to the bending motion of the valve in response to the same fluid load.

For a cantilever beam bending, it is a reasonable assumption and simplification that the the fluid force is concentrated at the center of the flow channel as shown in Figure 3(b) because the valve opening is small. Under this assumption, the deflection at the opening is given by

$$y = \frac{Pa^3}{3EI} \tag{3}$$

where E is the modulus of elasticity, I is the area moment of inertia, P is the concentrated load and a is the distance from fixed end. For a small deflection, we can have $\theta = arctan(\frac{y}{a}) \simeq \frac{y}{a}$. Coupled with the torque $T = Pa$, the torsion coefficient becomes:

$$K = \frac{T}{\theta} = \frac{Pa^2}{y} = \frac{3EI}{a} \tag{4}$$

Once K and I are determined, Equation (1) can be solved for reed valve dynamics. The generation and moving/deforming of the reed valve mesh is handled by *Circumferential Valve* template which is built into Simerics-MP+ software package.

4. CFD solver and governing equations

The conservation of mass, momentum, and energy of a compressible fluid are solved using finite volume method. These conservation laws can be written in integral representation as

$$\frac{\partial}{\partial t}\int_{\Omega(t)} \rho d\Omega + \int_\sigma \rho(\mathbf{v} - \mathbf{v}_\sigma)\cdot\mathbf{n}d\sigma = 0 \tag{5}$$

$$\frac{\partial}{\partial t}\int_{\Omega(t)} \rho\mathbf{v}d\Omega + \int_\sigma \rho((\mathbf{v} - \mathbf{v}_\sigma)\cdot\mathbf{n})\mathbf{v}d\sigma = \int_\sigma \tau\cdot\mathbf{n}d\sigma - \int_\sigma p\mathbf{n}d\sigma + \int_\Omega \mathbf{f}d\Omega \tag{6}$$

$$\frac{\partial}{\partial t}\int_{\Omega(t)} \rho E d\Omega + \int_\sigma \rho((\mathbf{v} - \mathbf{v}_\sigma)\cdot\mathbf{n})Ed\sigma = \int_\sigma \kappa\nabla T\cdot\mathbf{n}d\sigma - \int_\sigma p\mathbf{v}\cdot\mathbf{n}d\sigma + \int_\sigma (\mathbf{v}\cdot\tau)\cdot\mathbf{n}d\sigma + \int_\Omega \mathbf{f}\cdot\mathbf{v}d\Omega \tag{7}$$

in which $\Omega(t)$ is the volume of the computational domain or control volume, σ is the surface of $\Omega(t)$, $\mathbf{n}$ is the surface normal of σ pointed outwards, ρ is the fluid density, p is the pressure, $\mathbf{f}$ is the body force, $\mathbf{v}$ is the fluid velocity and $\mathbf{v}_\sigma$ is surface motion velocity. The shear stress tensor τ is a function of the fluid viscoty μ and the velocity gradient.

The standard $k-\epsilon$ two-equation model [17] is used to account for turbulence,

$$\frac{\partial}{\partial t}\int_{\Omega(t)} \rho\kappa d\Omega + \int_\sigma \rho((\mathbf{v} - \mathbf{v}_\sigma)\cdot\mathbf{n})\kappa d\sigma = \int_\sigma (\mu + \frac{\mu_t}{\sigma_\kappa})(\nabla\kappa\cdot\mathbf{n})d\sigma + \int_\Omega (G_t - \rho\epsilon)d\Omega \tag{8}$$

$$\frac{\partial}{\partial t}\int_{\Omega(t)}\rho\epsilon d\Omega+\int_{\sigma}\rho((\mathbf{v}-\mathbf{v}_{\sigma})\cdot\mathbf{n})\epsilon d\sigma=\int_{\sigma}(\mu+\frac{\mu_t}{\sigma_{\epsilon}})(\nabla\epsilon\cdot\mathbf{n})d\sigma+\int_{\Omega}(c_1G_t\frac{\epsilon}{\kappa}-c_2\rho\frac{\epsilon^2}{\kappa})d\Omega \quad (9)$$

Together with equation of state, where properties are functions of temperature and pressure, to form a closed system:

$$\rho=f(p,T) \quad (10)$$

5. Case Setup

The novel rotary compressor with gas injection system proposed by Wang *et al.* [11] includes the suction port, rotor, discharge port and gas injection port as shown in Figure 4. The rotary piston chamber and discharge ports are connected via two discharge reed valves. The gas injection port is connected to the rotary piston chamber through a reed valve which moves with the vane. The working principles of the gas injection structure are discussed in details in [11]. The fluid volumes are meshed using a binary tree unstructured mesh except the valve and rotor volumes which are meshed through templates *Rolling Piston* and *Circumferential Valve*, respectively. The total number of cells is about 1.3 million. Two adjustable leakage channels are included in the model, which are at the vane tip and the contact region between the piston and the chamber wall.

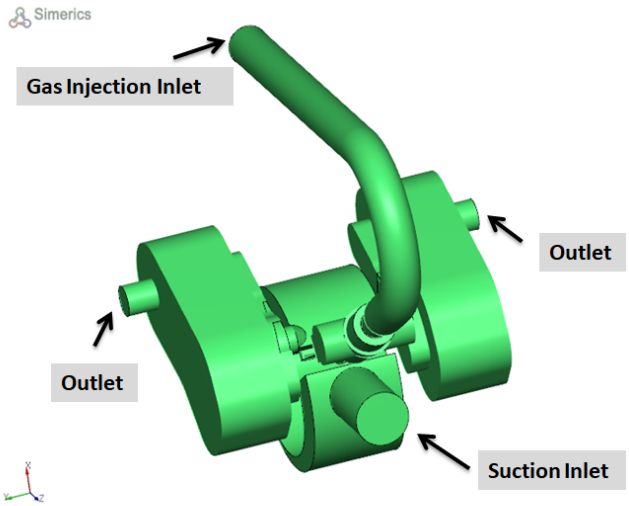

Figure 4. Fluid domain for a rotary compressor with gas injection system

Fixed total pressure and temperature are specified at the suction and gas injection inlets. The discharge outlets are assigned a constant pressure. The refrigerant in the system is R22. Various operation conditions are listed in Table 1.

In Table 1, P_{in} is the inlet pressure, T_{in} is the inlet temperature, $P_{in}^{'}$ is the gas injection inlet pressure, $T_{in}^{'}$ is the gas injection inlet temperature, P_{out} is discharge outlet pressure and f is the rotating frequency.

Various suction and gas injection inlet pressures and temperatures are specified in Case1 - 8 in which the reed valve in gas injection system can open to allow the gas to flow into the

Table 1. Operating conditions

Cases	P_{in} (kPa)	T_{in} (C)	$P_{in}^{'}$ (kPa)	$T_{in}^{'}$ (C)	P_{out} (kPa)	f (Hz)
1	296.2	15	655	10.72	1729.2	50
2	584.1	15	985	24.86	1729.2	50
3	245.31	-15	587	7.16	1729.2	50
4	354.79	-5	730	14.33	1729.2	50
5	497.99	5	890	21.21	1729.2	50
6	640.88	13	1039	26.83	1729.2	50
7	354.79	-5	730	14.33	1729.2	30
8	354.79	-5	730	14.33	1729.2	70
9	296.2	15	200	-20	1729.2	50
10	584.1	15	200	-20	1729.2	50
11	245.31	-15	200	-20	1729.2	50
12	354.79	-5	200	-20	1729.2	50
13	497.99	5	200	-20	1729.2	50
14	640.88	13	200	-20	1729.2	50
15	640.88	13	–	–	1729.2	50

pump chamber. On the contrary, the gas inject inlet pressures and temperatures in Case9 - 14 are specified sufficient low to keep the reed valve in the gas injection system closed during the operation. In Case15, the gas injection system is removed, but the volume adjacent to the rolling chamber is kept.

6. Results and Discussion

The motion of the discharge valve and the corresponding outlet mass flux predicted by the CFD simulation in Case3 are plotted in Figure 5. It is observed that the results are periodic between cycles. The discharge valve remains open for about 120 degree of the crank rotation with a maximum opening angle nearly 6 degrees. It is also seen that the discharge valve opens and closes very quickly due to the very low inertial of the discharge valve. The corresponding outlet mass flux plot shows the same pattern. Figure 6 shows the opening angle of the reed valve in the gas injection system and the corresponding mass flux which is also periodic. Due to a lower stiffness, the gas injection reed valve opens sharply and stays at the maximum opening angle (about 6 degrees) for nearly 140 degrees of the crank rotation. Gas flows into the piston chamber from the gas injection system when the reed valve is open. However, reverse gas flow (from the piston chamber to gas injection system) is also observed when the valve reaches its closing position although it only lasts a very short period. Valve dynamics and mass flow rates are also examined in other cases and they all exhibit periodic patterns.

In this study, the discharge outlet mass flow rate and the gas injection mass flow rate are extracted from CFD simulations and used to evaluate the performance of rotary compressor with the novel gas injection structure. The results are listed in Table 2 in which M is the discharge outlet mass flow rate, $M^{'}$ is the gas injection mass flow rate, M_{exp} is the mass flow rate measured in experiments and $M_{exp}^{'}$ is the gas injection mass flow rate measured in experiments.

Case1 and Case2 are baseline tests in which the discharge outlet mass flux and gas injection

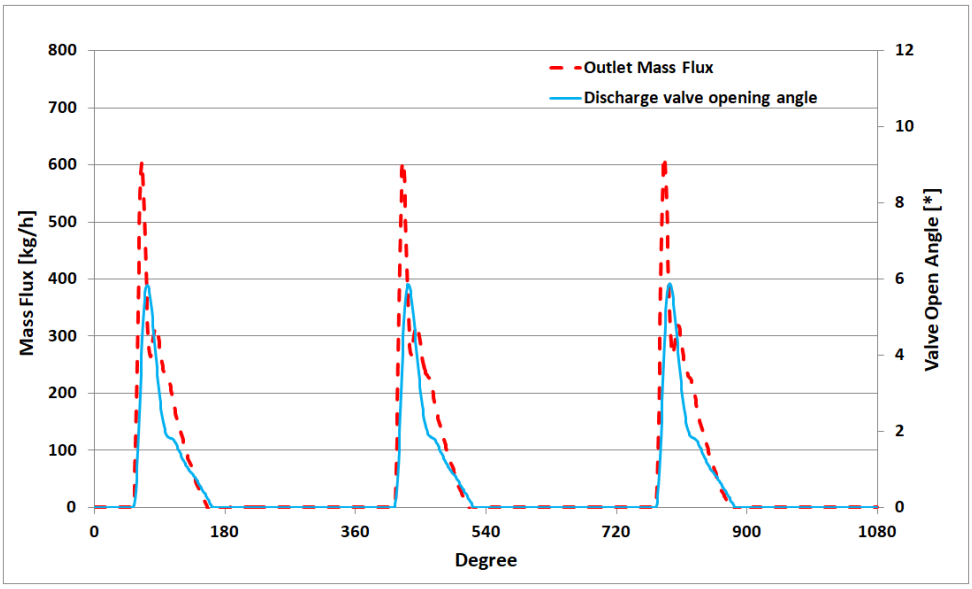

Figure 5. Outlet mass flux and discharge opening angle for Case3 over 3 cycles of compressor simulation

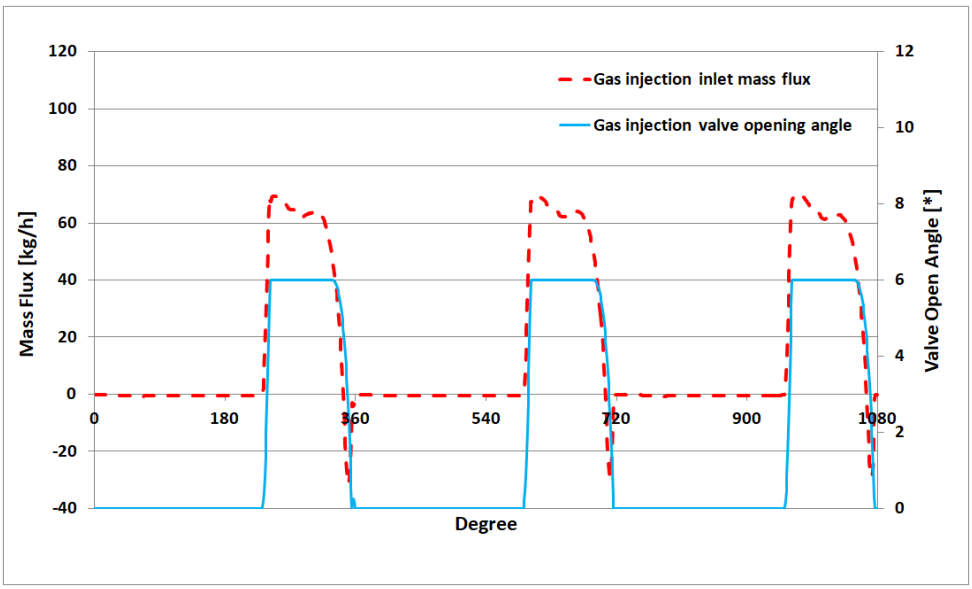

Figure 6. Gas injection inlet mass flux and valve opening angle for Case3 over 3 cycles of compressor simulation

inlet mass flux are measured in experiments. In Case1, the discharge outlet mass flux is predicted at 64.4 kg/h by CFD simulation and the difference is only about 1.2% comparing to 65.2 kg/h from the experiment. For the mass flux through gas injection inlet, CFD simualtion gives 16.5 kg/h which is slightly higher (3.5%) than the experimental data 16.0 kg/h. In Case2, the differences between the CFD simulation results and experimental measurements for the discharge outlet mass flux and gas injection inlet mass flux are 1.5% and 2.2% respectively. Thus, a good agreement between CFD simulations and experiments for the rotary compressor with gas injection system is achieved. With different boundary conditions, Case3-8 are carried

Table 2. Outlet mass flux in kg/h

Cases	M	$M^{'}$	M_{exp}	$M^{'}_{exp}$	Cases	M	$M^{'}$	M_{exp}	$M^{'}_{exp}$
1	64.4	16.5	65.2	16.0	9	51.7	0	51.1	0
2	131.3	17.6	133.3	18.0	10	116.5	0	116.4	0
3	58.4	16.6	–	–	11	45.3	0	–	–
4	83.2	17.1	–	–	12	69.7	0	–	–
5	115.8	17.6	–	–	13	100.5	0	–	–
6	147.3	18.1	–	–	14	131.7	0	–	–
7	51.0	16.6	–	–	15	132.2	0	–	–
8	115.9	17.9	–	–					

out using the same model settings as in Case1 and Case2.

The discharge outlet mass flow rates in experiments are also provided in Case9 and Case10. In Case9, it is observed that the discharge outlet mass flux 51.7 kg/h predicted by CFD simulation is close to 51.1 kg/h from the experiment with a difference about 1.2%. In Case10, the discharge outlet mass flux from CFD simulation agrees with the experimental test very well with a difference of 0.1%. Case11-14 are conducted using the same model settings in Case9 and Case10. By comparing the discharge outlet mass fluxes in cases with and without gas injection system, it can be seen that the refrigerant mass flow in the compressor system is significantly improved by the gas injection structure.

In Case15, the gas injection system is removed except the volume adjacent to the piston chamber. It is clear that there is no notable effect of that volume on the rotary compressor performance by comparing the discharge outlet mass flux (132.2 kg/h) from Case15 to that from Case14 (132.2 kg/h).

7. Summary and Conclusions

A 3D CFD, transient model of rotary compressor is presented in this work. The piston chamber motion are fully coupled with the reed valves by solving valve dynamics. The procedure to calculate the parameters for the dynamics fluid-structure simulation of the valve is outlined. Rolling piston chamber and valves are meshed using templates *Rolling Piston* and *Circumferential Valve* respectively. This 3D model is employed to carried out CFD simulations to study the rotary compressor with gas injection structure. A good agreement is achieved between CFD predictions and experimental data. It is found that the novel gas injection structure can effectively enhance the rotary compressor performance by increasing the refrigerant mass in the system. The volume adjacent to the piston chamber has no notable effect of the discharge outlet mass flow. Due to the template based meshing techniques and the robustness of flow solver, the setup and simulation is easy and fast. Simerics-MP+ can be readily applied to industrial compressor systems.

References

[1] Stefan, S.B., Eckhard A. G., 2005, Review of Air-source Heat Pumps for Low Temperature Climates, *8th International Energy Agency Heat Pump Conference*.

[2] S.G.Kim, M.S. Kim, Experimenta and simulation on the performance of an autocascade refrigeration system using carbon dioxide as a refrigeration, *International Journal of Refrigeration*, Vol. 25, pp. 1093-1101.

[3] Wang, B.L., Shi, W.X. and Li, X.T., 2009, Numerical analysis on the effects of refrigerant injection on the scroll compressor, *Applied Thermal Engineering*, Vol. 29, pp. 37-46.

[4] Ma, G.Y. and Chai, Q., 2003, Characteristics of an improved heat-pump cycle for cold regions. *International Journal of Regrigeration*, Vol. 26, pp.12-18.

[5] Wang, B., Shi, W., Han, L., 2009, Optimization of refrigerant system with gas-injection scroll compressor, *International Journal of Refrigeration*, Vol. 32, pp. 1544-1554.

[6] Heo, J., Jeong, M.W. and Baek, C., 2011, Comparison of the heating performance of air-source heat pumps using various types of refrigerant injection, *International Jounral of Regrigeration*. Vol. 34, pp. 444-453.
[7] Xu, S.X. and Ma, G.Y., 2014, Experiment study on two-stage compression refrigerant/heat pump system with dual-cylinder rolling piston compressor, *Applied Thermal Engineering*, Vol. 62, pp. 803-808.
[8] Ko,Y., Park, S. and Jin, S., 2013, The selection of volume ratio of two-stage rotary compressor and its effects on air-to-water heat pump with flash tank cycle, *Applied Engery*, Vol. 104, pp. 187-196.
[9] Jia, Q. L., Feng, L.W. and Yan, G., 2014, Experimental research on rotary compression system with vapor injection, *Refrigeration and Air Conditioning*, Vol.14, pp. 128-132.
[10] Jia, Q. L., Feng, L.W. and Yan, G., 2015, Experimental research on heating performance of rotary compression system with vapor injection, *Journal of Refrigeration*, Vol. 36, pp. 65-70.
[11] Wang, B., Liu, X. and Shi, W., 2016, A novel vapor injection structure on the blade for rotary compressor, *International Compressor Engineering Conference at Purdue*, Paper 1180,
[12] Geng, W., Liu, C., and Wang, Y., 2004, The Performance Optimization of Rolling Piston Compressors Based on CFD Simulation, *International Compressor Engineering Conference at Purdue*, pp. 1488-1492.
[13] Liang, S., Xia, S., Kang, X., Zhou, P., Liu, Q., and Hu, Y., 2010, Investigation of Refrigerant Flow Simulation and Experiment of Rolling Piston, *International Compressor Engineering Conference at Purdue*, Paper 1164.
[14] Machu, G.,; Albrecht, M., Bielmeier, O., Daxner, T., and Steinruck, P., 2004, A Universal Simulation Tool for Reed Valve Dynamics, *International Compressor Engineering Conference at Purdue*, Paper 1716.
[15] Silva, E., Deschamps, C. J., and Fancello , E. A., 2012, A Procedure to Optimize Reed T ype V alves Considering Efficiency and Bending Fatigue, *International Compressor Engineering Conference at Purdue*, Paper 2106.
[16] Kinjo, K., Nakano, A., Hikichi, T., and Morinishi, K., 2010, Study of CFD Considering Valve Behavior in Reciprocating Compressor, *International Compressor Enngineering Conference at Purdue*, Paper 1975.
[17] Launder, B.E., and Spalding, D.B., 1974, The numerical computation of turbulent flows, *Comput. Methods Appl. Mech. Eng.*, Vol. 3, pp. 269-289.
[18] Ding, H. and Gao, H., 2014, 3-D Transient CFD Model for A Rolling Piston Compressor with A Dynamic Reed Valve, *22nd International Compressor Engineering Conference*, Paper 1548.